Developments in the Built Environment 16 (2023) 100286

Contents lists available at ScienceDirect

Developments in the Built Environment

journal homepage: www.sciencedirect.com/journal/developments-in-the-built-environment

Development of improved porous asphalt mixtures with high porosity levels

Carlos J. Slebi-Acevedo [a], Pedro Lastra-González [b,*], Irune Indacoechea-Vega [b], Daniel Castro-Fresno [b]

[a] Escuela Colombiana de Ingeniería Julio Garavito. Centro de Estudios Geotécnicos, Bogotá, Colombia
[b] GITECO Research Group, Universidad de Cantabria, Av. de los Castros 44, 39005, Santander, Spain

ARTICLE INFO

Keywords:
Porous asphalt
Polymer modified binder
Porosity
Fibers
PCA
AHC

ABSTRACT

Porous asphalt (PA) mixtures are gaining wider acceptance in pavement construction due to their benefits in terms of road safety, noise mitigation and stormwater management. Increasing demands, such as those imposed by climate change, require the design of mixtures that provide enhanced functional properties, while keeping the same durability of conventional porous asphalt mixtures. This study proposes different experimental PA mixes with higher air voids content and suitable structural capability than a conventional PA mixture. The functionality of the mixtures was evaluated in accordance with total and interconnected air voids, while the mechanical performance was assessed in terms of raveling resistance both in dry and wet conditions, tensile strength, and moisture sensitivity. The binder drain down was also verified. In a first stage, the experimental results were analyzed through descriptive and inferential statistics tests. As multiple responses were obtained, principal component analysis (PCA) and agglomerative hierarchical clustering (AHC) were applied to explore the association pattern among the test results and experimental designs. The study concluded that PA mixes with air voids content of up to approximately 28% and admissible values of resistance can be designed. The use of polymer modified binder (PMB) and the inclusion of fibers and hydrated lime (HL) was essential for the formulation of the mixes.

1. Introduction

Given the high rate of urbanization in cities, the area of impervious surfaces is increasing the risk of negative impacts on the environment such as flooding (Hammes et al., 2018). In addition, climate change, together with the growth of the automobile fleet, requires the development of infrastructures that are not only more resistant but also more sustainable. The use of porous asphalt (PA) mixture as wearing course has emerged as a popular solution to help address the increased demands of stormwater management. This mixture produced with low quantity of fines has high porosity, allowing the drainage of water through its structure improving the surface runoff. Other benefits reported in the literature include the mitigation of the tire-pavement noise, high skidding resistance, capability to dissipate splash and spray while driving on rainy days, reduction of glare while driving at night. and prevention of the hydroplaning phenomenon (Gupta et al., 2019; B. Xu et al., 2016).

The PA mixture was incorporated in Europe and America in the mid-1960s to increase the friction in the highways and hence to improve the safety of roads (Chen et al., 2018). In Netherlands more than 90% of the highway network is covered by PA for the purpose of reducing noise (Nielsen, 2006). Previous studies suggest that PA can decrease the average noise level of 3–4 dB (Liu et al., 2016). Besides, PA mixture gained recognition in the world of sustainable drainage systems (SUDS) as a surface layer of a permeable pavement system (PPS), through which the amount of surface runoff is minimized by helping the water penetrate through its structure (Gupta et al., 2019). The open-graded structure and the large air voids content produce its functional advantages. In the United States typical air voids content varies from 18% to 22% while in Europe it is around 20% (Alvarez et al., 2011). It is worth mentioning that the porosity of the PA has a direct influence on the durability of the mixture. Thus, the presence of high voids content usually results in a lower service life expectancy as compared to dense-graded asphalt mixtures. Raveling, the loss of coarse aggregates from the road surface due to the abrasive loads of the traffic, is the most common type of failure observed in the PA mixtures (Manrique-Sanchez et al., 2018).

* Corresponding author.
E-mail addresses: Carlos.slebi@escuelaing.edu.co (C.J. Slebi-Acevedo), pedro.lastragonzalez@unican.es (P. Lastra-González), irune.indacoechea@unican.es (I. Indacoechea-Vega), castrod@unican.es (D. Castro-Fresno).

https://doi.org/10.1016/j.dibe.2023.100286
Received 31 August 2023; Received in revised form 8 November 2023; Accepted 20 November 2023
Available online 25 November 2023

This phenomenon normally occurs because of poor adhesion in the binder-aggregate interface or the loss of cohesion within the asphalt mortar (Adam et al., 1998; Mo et al., 2011). The high porosity exposes the bituminous binder to higher rates of oxidation and moisture damage weaking the binder's ability to bond the aggregates effectively, potentially compromising the cohesive strength of the mixture (Huurman et al., 2010).

Clogging is another important problem of the PA mixtures in terms of functionality. It happens when the pores are blocked by the dust and fine materials affecting directly the permeability and the infiltration rate of the pavement (Garcia et al., 2019). According to Chen et al. clogging accelerates the freeze-thaw deterioration cycles because of the additional water retained in the pores (Chen et al., 2018). Moreover, as the porosity and permeability of the PA increases, the influence of clogging is lower (Ranieri et al., 2011).

Multiple additives and modifiers have been incorporated into the PA mixture to increase its structural capability; these include fibers, polymers, modified binders and alternative fillers (Slebi-acevedo et al., 2020). Overall, polymer modified binder (PMB) is the most common alternative to be applied as binder in the PA since it provides greater elastic recovery and higher ductility (Rogers et al., 2019). In the US, PMB and rubber-modified binders are preferred over conventional binders to achieve a more durable PA pavement (Ma et al., 2018). The addition of polymers such as crumb rubber (CR) and styrene-Butadiene-Styrene (SBS) to manufacture high viscosity binders also increases the engineering properties of the bitumen reducing moisture-induced raveling damage (Ren et al., 2021). Fibers are also added to increase the mechanical performance of the mixture. Many studies have reported increments in the tensile strength, fracture energy properties and toughness with fiber addition (Gupta et al., 2019; Park et al., 2015; Q. Xu et al., 2010). Similarly, fibers can act as a barrier preventing the formation and propagation of cracks (Park et al., 2015). In PA and Stone matrix asphalt (SMA) adding fibers is a good solution to avoid the binder drain down and hence to stabilize the mix (Abtahi et al., 2010). Among the fillers, the hydrated lime (HL) is an excellent additive to prevent the moisture damage. Previous studies have reported that HL reduces the chemical aging of the bitumen, and enhancements in the strength and modulus have been observed in mixes modified with this additive (Mohd Shukry et al., 2018). In fact, these positive observations have led the Netherlands to implement HL in the production of their PA mixes.

In a previous research the authors of this study used design of experiments (DOE) combined with a multi-criteria decision making analysis (MCDMA) (Slebi-Acevedo et al., 2021) to select the most promising additives that can be applied in a PA mixture. The modifiers evaluated included the PMB as binder, synthetic fibers, and HL as replacement of the filler. The main purpose of this research is to develop an enhanced porous asphalt mixture with higher air voids content and a structural capacity suitable and similar to a conventional PA mixture. Various experimental PA mixes with different empirical gradations curves and modified with additives were assessed to increase the air voids of the mixture and maintain a proper durability. As part of the evaluation, both total and interconnected air voids were determined. Besides, the testing protocol encompassed binder drain down, particle loss under both dry and wet conditions, indirect tensile strength, and moisture susceptibility.

Descriptive statistics were used to describe and explore the basic features of the dataset, whereas inferential statistics were conducted for comparison purposes among the experimental designs. Additionally, in this study, principal component analysis (PCA) and agglomerative hierarchical clustering (AHC) were included as promising exploratory techniques to evaluate the degree of interrelation among the mixtures and to observe the multiple association between the responses recorded. Both methods are useful when analyzing numerous mixture designs with multiple response variables simultaneously. On the one hand, PCA allows to establish groups of inter-related responses, to reduce the number of variables and to convert them into principal components (PCs) which contain information about the contribution of the total variance of the data set. On the other hand, AHC facilitates the classification of the experimental designs based on their similitudes with respect to the scores found in the PCs. These statistical tools have been applied in many fields such as biology (Elshamy et al., 2019), sustainability (Canal & Delta, 2020), energy (Burgas et al., 2021) and food sciences (Cadot et al., 2012). In civil engineering studies, Bouyad and Emeriault (Bouayad and Emeriault, 2017), applied PCA and AHC methods to describe the association pattern between the tunnel boring machines (TBM) parameters and geology profiles. In another study, soil spatial patterns at the ancient city of Ibida (Northerm part of Dobrogea, Romania), were identified by PCA and AHC multivariate statistical methods (Gabriel et al., 2020). Tidjani et al. (2020) employed AHC to identify road infrastructures that could have an impact on the degradation of the road markings. Related to bituminous binders, Margaritis et al. (2020) applied the same analytical method to classify reclaimed asphalt binders belonging into similar aging states, on a chemo-rheological basis. As far as the authors of this research know, the combination of these exploratory techniques has not been used before, to investigate multiple responses in the field of porous asphalt mixtures. Accordingly, with PCA and AHC the aim is to make an exploratory analysis of the multiple data set and establish correlations between the experimental response variables and classify the observations based on their similarities in relation to their physical properties.

2. Materials and methods

2.1. Materials

For the preparation of the specimens two types of bituminous binder were employed: the virgin bitumen 50/70 penetration-grade and a polymer modified binder. Their main characteristics are listed in Table 1.

Concerning aggregates, ophite with a specific gravity of 2.787 g/cm^3 was employed as the coarse fraction while limestone with a specific gravity of 2.705 g/cm^3 was used as the fine fraction and filler material. To improve the bonding of the bitumen, HL content of 25 percent was incorporated as replacement of the filler in the experimental mixtures. Their physical properties are presented in Table 2.

Two types of synthetic fibers were used as reinforcement and binder stabilizer of the experimental mixes. The first one corresponded to a set of polyolefin-aramid (POA) fibers. On the one hand, aramid fiber is characterized for having an elevated tensile strength and high thermal resistance as compared to other type of synthetic fibers (polypropylene, polyester, polyacrylonitrile). On the other hand, polyolefin fiber acts well as a dispersing agent avoiding the formation of clusters in the mix. Additionally, polyolefin has a similar melting point than the binder and, hence, it can work as a bitumen modifier. Previous studies have shown good results with the addition of POA fibers (Fazaeli et al., 2016; Gupta et al., 2021; Slebi-acevedo et al., 2020). The length of both fibers is 19 mm and the density of the set determined according to the European standard method EN 1097–6 was 0.95 g/cm^3.

Table 1
Characteristics of bituminous binders. Virgin Binder (VB), polymer modified binder (PMB).

Test	Standard	Binder	
		VB	PMB
Penetration (25 °C, dmm)	EN 1426	57	55
Specific Gravity	EN 15326	1.04	1.03
Softening point (°C)	EN 1427	51.6	74.1
Fraass brittle point (°C)	EN 12593	−13	−13
Ductility force (5 °C, J/cm^2)	EN 13589	–	3.11
Elastic recovery (25 °C, %)	EN 13398	–	92

Table 2
Physical properties of the aggregates.

Ophite - coarse aggregate fraction			
Property	value	specification	Normative
Los Angeles coefficient	13	≤20	EN 1097-2
Specific weight (g/cm3)	2.787	–	EN 1097-6
Polished stone value (PSV)	60	≥56	EN 1097-8
Flakiness Index (%)	8	≤20	EN 933-3
Limestone - fine aggregate fraction and filler material			
Property	value	specification	Normative
Los Angeles coefficient	28	<25	EN 1097-2
Specific weight (g/cm3)	2.705	–	EN 1097-6
Sand equivalent	78	>55	EN 933-8
Hydrated lime - as replacement of the filler material			
Property	value	specification	Normative
Specific weight (g/cm3)	1.959	–	EN 1097-6
CaO content (%)	>90%	–	–

The second fiber selected as reinforcement was aramid pulp (Pulp), which is a type of fibrillated chopped aramid fiber that has been used as a reinforcement in other composites such as carbon-fiber-reinforced plastics (CFRP) (Hu et al., 2020; Lertwassana et al., 2019). Like conventional aramid fibers, Pulp has high thermal resistance as well as high tensile strength properties. Unlike conventional aramid fiber, which is a thin filament fiber, Pulp fibers have stratified small branches with fibrillary surfaces. Due to the particular shape, this fiber provides high wearing resistance, large frictional properties, and hence can be easily adhered to other polymeric binders (Lertwassana et al., 2019). The length of the Pulp fiber is approximately 1.15 mm. Pictures of the types of fibers used in the current research are presented in Fig. 1.

2.2. Experimental designs

A total of eleven PA mixtures, in addition to those deemed as reference mixtures, with different aggregate gradations were designed for this study (see Table 3). The main purpose of the experimental design is to obtain a PA mixture with high air voids content while keeping a suitable mechanical performance.

A typical gradation curve from Spain with a maximum particle size of 16 mm was taken as control gradation to design four additional empirical gradation curves, as shown in Fig. 2. It is worth mentioning that PA16 was chosen to allow a thick layer to improve the infiltration capabilities of the road. Each one of the gradations was designed to increase the air voids and improve its functional capabilities. Gradations number three and four were expected to have the highest porosity while the gradation number one was expected to have the lowest one. The designs of the mixtures were done sequentially, trying to improve the mechanical performance of the previous one. Two reference mixtures with virgin and polymer modified binder were manufactured for comparison with the experimental mixtures. Both mixtures were formulated to achieve a 20% porosity with a binder content of 4.50%, ensuring no risk of binder drain down. Similarly, reference mixtures were prepared using conventional filler. With respect to the experimental mixes, despite having fewer fine aggregates to increase the air voids, they were designed with a higher bitumen content. This was possible because the fibers not only act as reinforcement in the mixture but also absorb bitumen preventing its leakage.

Table 3
Empirical PA mixtures with high infiltration capabilities.

Mixture ID	Binder type	Binder content (%)	Gradation used	Fiber type	Fiber content (%)
REF 1	50/70	4.50	Control	–	–
REF 2	PMB 45/80 - 65	4.50	Control	–	–
PA 1	PMB 45/80 - 65	5.00	1	Pulp	0.05
PA 2	PMB 45/80 - 65	5.00	1	POA	0.05
PA 3	PMB 45/80 - 65	5.00	1	Pulp	0.08
PA 4	PMB 45/80 - 65	5.00	2	Pulp	0.05
PA 5	PMB 45/80 - 65	5.00	3	Pulp	0.05
PA 6	PMB 45/80 - 65	5.00	3	POA	0.05
PA 7	PMB 45/80 - 65	5.00	3	POA	0.15
PA 8	PMB 45/80 - 65	5.00	4	POA	0.15
PA 9	PMB 45/80 - 65	5.00	4	Pulp	0.05
PA10	PMB 45/80 - 65	5.30	3	Pulp	0.05
PA11	PMB 45/80 - 65	5.30	3	POA	0.15

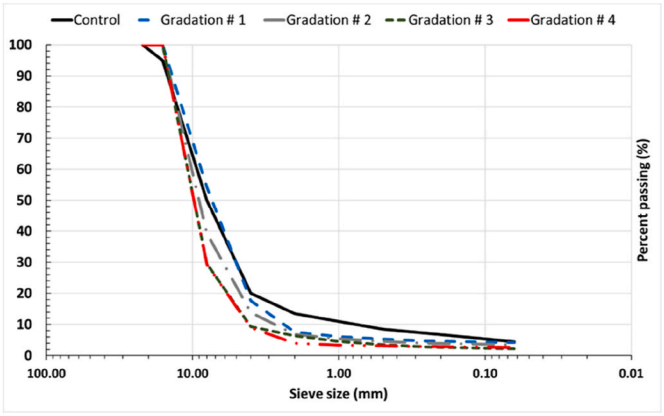

Fig. 2. Particle size distributions used in the current study.

Fig. 1. Illustration of the fibers used as reinforcement. (a) POA fibers; (b) Pulp fibers.

2.3. Specimen preparation

The preparation of specimens was done following a traditional procedure. Initially the coarse and fine aggregates, as well as filler material, were heated and blended to meet the requirements of the gradations proposed. Then fibers were added by dry method, which means prior to the addition of bitumen. Once a homogeneous mixture was reached, the binder was incorporated into the fiber-aggregate matrix and mixed continuously. In the mixture prepared with virgin binder the mixing temperature was 170 °C while in the designs manufactured with PMB the manufacturing temperature was 165 °C. Cylindrical specimens were compacted using the standard Marshall compaction method and applying 50 blows on each face following the EN 12697-34 standard.

2.4. Experimental set-up

The experimental tests carried out in this research are presented in Table 4. The total and interconnected air voids were determined based on their volumetric properties according to European Standard EN 12697–8 and used as indicator of the functional performance of the PA mixtures. Additional insights can be found in (Slebi-Acevedo et al., 2022). A higher content of total voids means a higher permeability and infiltration rate (Alvarez et al., 2011). The particle loss Cantabro test developed in the 1990s in Spain (Arrieta and Maquilón, 2014; Calzada-Perez and Perez-Jimenez, 1984) was conducted on cylindrical specimens to evaluate the raveling resistance of compacted mixes. In the test, the samples are conditioned in a climatic chamber at 15–25 °C, their initial weight is recorded to afterwards being submitted to the Los Angeles Machine without abrasive load for 300 revolutions at 30 rpm. The particle loss (PL) expressed in percentage is calculated as the ratio of lost weight from the initial weight of the compacted sample. In addition, the test was also carried out in wet conditions following the Spanish Standard NLT 362/92. In this case, the samples are initially submerged in a water bath at 60 °C for 24 h and then disposed in a climatic chamber at 25 °C for another 24 h prior to perform the test as described in the dry condition.

Additionally, the indirect tensile strength (ITS) and the moisture sensitivity of the PA mixes were assessed as other criteria of durability. To carry out with the test, a total of eight samples are required to be divided in two groups of four samples each one. The first group corresponded to dry samples, which were stored in a climatic chamber at 15 °C. Meanwhile, the second denoted as wet samples were kept in a water bath at 40 °C for 68–72h. Finally, the samples are disposed during 3 h at 15 °C before carrying out the ITS test according to EN 12697 - 23. Finally, the potential for moisture induced damage is measured in terms of the indirect tensile strength ratio (ITSR). The ITSR is computed as the ratio of the wet ITS (ITS_{wet}) to the dry ITS (ITS_{dry}), expressed in percentage.

Finally, as the experimental mixtures have low fines, the mesh basket binder drain down test was performed to check the binder stability at high temperatures according to EN 12697–18. This test displays the amount of binder drainage relative to the total weight of the mixture. According to previous studies found in the literature, the binder drain down must not exceed 0.3% by weight of the total mix (Lyons and Putman, 2013; Putman et al., 2012).

Table 4
Experimental tests.

Response	Symbol	units	Standard	Comments	Replicates
Total air voids	T_{AV}	%	EN 12697 - 8	Volumetric properties	16
Interconnected air voids	I_{AV}	%	–	Volumetric properties	4
Particle loss - dry conditions	PL_{dry}	%	EN 12697 - 17	European standard	4
Particle loss - wet conditions	PL_{wet}	%	NLT 362/92	Spanish standard	4
ITS - dry conditions	ITS_{dry}	kPa	EN 12697 - 23	European standard	4
ITS - wet conditions	ITS_{wet}	kPa	EN 12697 - 12	European standard	4
Moisture sensitivity	ITSR	%	EN 12697 - 12	European standard	8
Binder drain down	BD	%	EN 12697 - 18	European standard	2

2.5. Statistical analysis

The experimental results obtained from the laboratory tests were examined by using descriptive, inferential, and exploratory statistics. Descriptive statistics was used to inquire into the features of the experimental designs. Some statistical measures like mean, median, standard deviation as well as the upper and lower quartiles were recorded and graphed in box and whisker plots. Similarly, histograms were examined, and the normality of the data was checked through the Anderson-Darling normality test and the homogeneity of variance was compared by the Levene's test. Depending on the data distribution and homoscedasticity, inferential statistics were applied for comparison purposes among the designs. One-way analysis of variance (ANOVA) parametric test was employed in those cases where the data were normally distributed and with homogeneity of variance. Otherwise, the Kruskal-Wallis non-parametric test was used. Similarly, multiple pairwise comparison tests were carried out for classification purposes. The confidence level of the statistical analysis was established in 95%. Accordingly, a p-value lower than 0.05 suggests the existence of statistically significant differences. Moreover, the statistical association between the different responses were investigated using the Pearson's correlation coefficient.

As many responses were obtained from the experimental designs, exploring and clustering data analysis were also done to concentrate the large amount of information into few representative dimensions and to clustering data based on the similarities found among the experimental designs. Consequently, the unsupervised exploratory statistical methods denoted as Principal Component Analysis (PCA) and Agglomerative Hierarchical Clustering (AHC) Analysis were employed respectively to that purpose.

As exploratory technique, PCA helps to analyze quantitative data which is organized in matrix form with X individuals and Y response variables. Through the method, the relationship between the response variables is quickly envisioned as well as the similarities between the individuals (Tidjani et al., 2020). Overall, PCA seeks to identify links between the data set to then project it on a reduced dimensional map. As the response variables were measured in different orders of magnitude, in PCA, each variable is firstly standardized by reducing and centering all the variables on the same scale. PCA looks to capture orthogonal dimensions based on linear combinations of the variables with the maximum variability of data. It is worth mentioning that the first dimension captured has the highest variability of the data while the other ones capture the remaining maximum variability in descendent order. As the main objective of PCA is dimensionality reduction, it is expected to capture the maximum variability of data with just two dimensions. Consequently, the 80% variance criterion is deemed, which means that the cumulative variability of two of the total dimensions should be higher than 80%.

AHC helps to cluster observations into sets of similar observations. This method is based on the concept of distance or dissimilarity between observations in relation to the measured variables. Like PCA, the observations are initially centered and reduced to standardized response variables. Next, the clustering of the observations is determined by computing the geometric Euclidean distance between them. The groups are typically showed in an attractive visual way called a dendrogram. Through the dendrogram, the branches contained explained the similarities found among the observations. Accordingly, larger distances

between the branches depicted higher dissimilarities between the experimental designs. The Wards or minimum variance linkage method was the criterion chosen to merge the pair of clusters at each step.

3. Results and discussion

3.1. Binder drain down results

Firstly, the binder drain down was verified among all the experimental designs (Table 5). Despite the small fine content in the mixtures, none of the mixtures exceeded the maximum admissible value of 0.3% recommended. It is hypothesized that, as expected, the addition of fibers contributed to stabilize the high content of binder in the mixture, thus preventing its leakage.

3.2. Total and interconnected air voids

The total and interconnected air voids of the experimental designs are displayed in the box and whisker plots in Figs. 3 and 4, respectively. In descriptive statistics, the box plots are very useful as they present the different quartiles, the interquartile range and outliers contained in the data set. The blue crosses indicate the mean values of the designs and the mean central bars the medians. The first and third quartiles are represented as the lower and upper limits of the box plot, respectively. The points above or below the whiskers are the outliers found in the replicates. Good replicability was obtained in the test with minimal outliers. As it can be expected, gradation curves three and four produced the highest voids among all PA mixtures. From designs 5 to 11, they presented the highest total and interconnected porosity. The total air voids ranged between 27 and 28%, whereas the interconnected porosity oscillated between 22 and 23%. For both responses, the data were normally distributed and with homogeneity of variance. Accordingly, the Tukey pairwise comparisons tests were done for grouping the samples as it can be seen in the Demsar plots (see Fig. 3b and 4b). In the Demsar plot, mixtures are ranked by their mean, and horizontal lines represent groups of mixtures with no statistically significant performance differences as determined by the Tukey test. Mixtures not connected by a line have means deemed significantly different. The results showed that the designs were divided in five groups for total and interconnected porosity. The experimental designs contained in each group indicate that there are no statistical differences between them. In that sense, it is worth mentioning that there were not statistical differences from design five to eleven. As consequence, in this study different PA mixtures with air voids content of approximately 28% and interconnected porosity of approximately 22% were reached.

In the same way, a high correlation was found between total and connected air void responses, as it can be observed in Fig. 5. A linear regression model with an R^2 value of 96% was obtained plotting the experimental results in the same graph. Accordingly, it can be concluded that either parameter is a good indicator of the functionality of the mix.

3.3. Particle loss Cantabro test results

As mentioned previously, raveling resistance is an important factor to measure the durability of the PA since this is the typical type of failure observed in these mixtures. Fig. 6 and Fig. 7 summarizes the results attained from the Cantabro test in dry and wet conditions, respectively. Given that the data exhibited heteroscedasticity across both responses, the Kruskal-Wallis test was selected to analyze the statistical differences. Concerning particle loss measured in dry conditions, all experimental

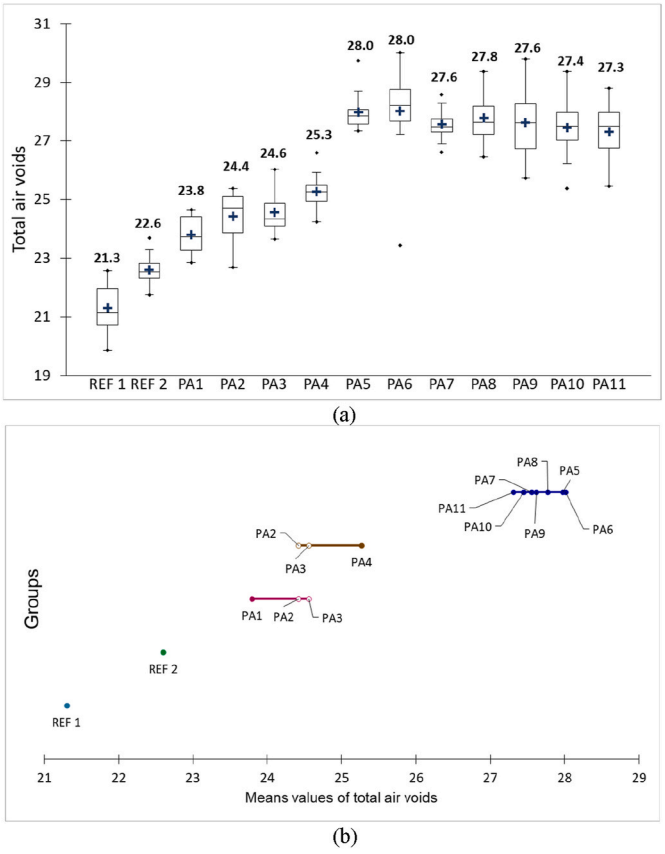

Fig. 3. Total air voids results; box and whiskers plot (a); Demsar plot (b).

designs yielded admissible values except mixtures PA8 and PA9, whose particle loss slightly exceeded 20%, the maximum recommended for the highest traffic level according to Spanish standards. Multiple pairwise comparisons among the samples were done using the Steel-Dwass-Critchlow-Fligner procedure to identify means that are significantly different from each other. It was observed that the mean values can be divided in two groups (see Fig. 6). Despite of the high voids content of the mixtures PA10 and PA11, no statistically significant differences were observed with respect to the reference mixtures. Besides, the PA7 with a void content of approximately 28% showed the highest raveling resistance with a particle loss at dry conditions of 10%, a value similar to the reference mixture with PMB. Based on the above, it can be said that the presence of aramid synthetic fibers was crucial as reinforcement in the mixes to keep a proper durability.

Concerning the results for wet conditions, a maximum value of 35% is admissible according to Spanish regulations. All the designs underwent particle losses lower than 35% except from PA6 which displayed a value of 39.1%. From the results it is clearly observed that the voids content has greater influence in the raveling resistance when wet. Designs PA1, PA3, PA4, PA7 and PA10 displayed lower values of particle loss as compared to REF1. However, designs PA7 and PA10 are the ones of greatest interest since they have higher porosity. Based on the multiple pairwise comparisons, PA10 and PA7 are grouped with REF1 and REF2 mixtures suggesting that not statistical differences are observed. From the results it can be inferred that it is possible to obtain a mixture with a high content of voids and maintain a durability similar to a

Table 5
Binder drain down results.

Design	REF 1	REF 2	PA1	PA2	PA3	PA4	PA5	PA6	PA7	PA8	PA9	PA10	PA11
BD (%)	0.00	0.00	0.00	0.00	0.00	0.00	0.00	0.08	0.00	0.00	0.00	0.00	0.07

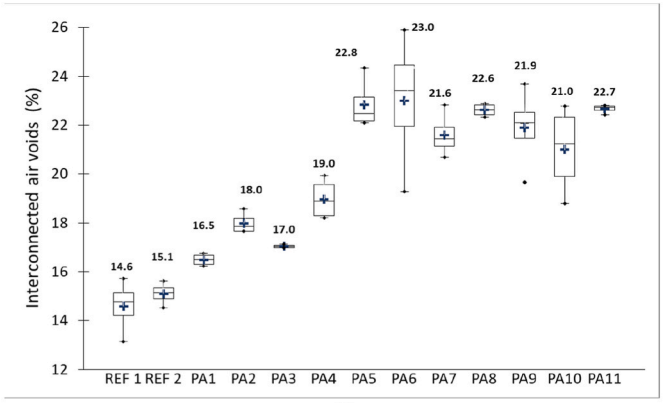

(a)

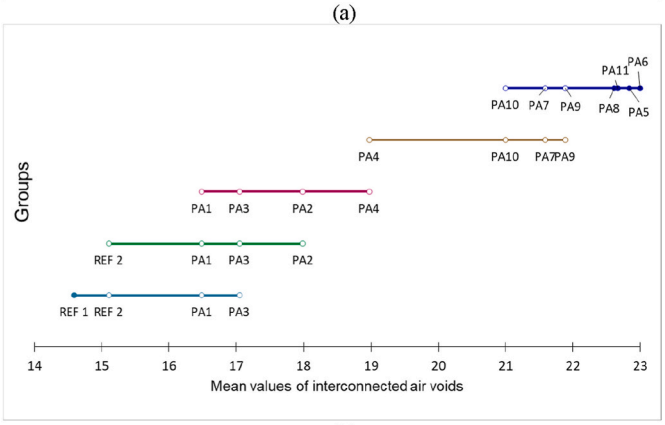

(b)

Fig. 4. Interconnected air voids results; box and whiskers plot (a); Demsar plot (b).

conventional PA mixture in terms of raveling resistance. In the same way, the addition of HL as replacement of the filler material could have a favorable impact on the wet strength of the mixtures. The inclusion of HL enhances the resistance of the asphalt to water stripping helping to maintain a suitable durability (Mohd Shukry et al., 2018).

3.4. ITS and water sensitivity test results

The ITS in both dry and wet conditions from all experimental designs, are illustrated in Figs. 8 and 9, respectively. From the results, it can be observed that as porosity increased, the tensile strength of the mixes was highly reduced. With regards to ITS in dry conditions response, the data were normally distributed with homoscedasticity and hence ANOVA test was carried out to investigate statistical differences. Designs PA1, PA2, PA3 with porosity content of 24% showed slightly lower tensile strength values than REF2 and close values to REF1. Moreover, it is worth highlighting that PA11 mixture with voids content of 28% depicted good performance in tensile resistance with no statistical differences with respect to reference mixtures. In relation to designs PA7 and PA10 with increased porosity and prepared with 0.15% and 0.05% of POA and AP fibers, respectively, they showed lower results of tensile strength as compared to reference mixture with virgin binder. However, the differences were not statistically significant, suggesting that a similar performance can be obtained compared to a conventional mix. Once again, the addition of aramid fibers had a direct positive effect on the reinforcement of the mix. In line with previous studies, aramid fibers have high tensile strength relative to asphalt mixture, and have the potential to increase the cohesion and tensile strength of the bituminous mixes (Abtahi et al., 2010; Gupta, Castro-fresno, et al., 2021; Slebi-Acevedo et al., 2020).

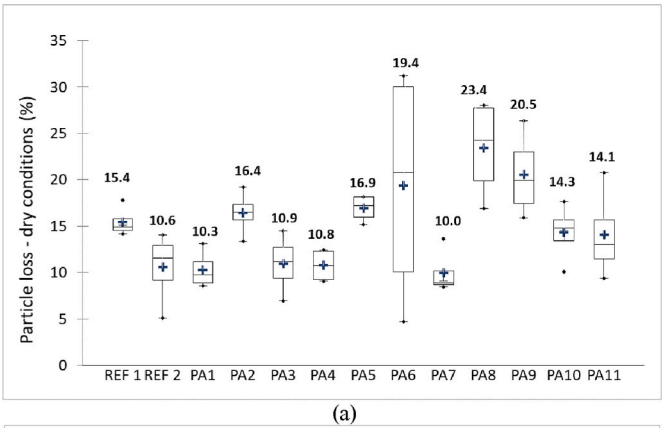

(a)

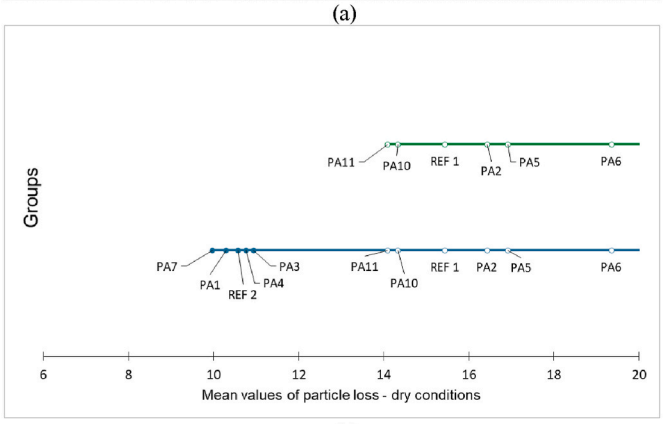

(b)

Fig. 6. Particle loss – dry conditions results; box and whiskers plot (a); Demsar plot (b).

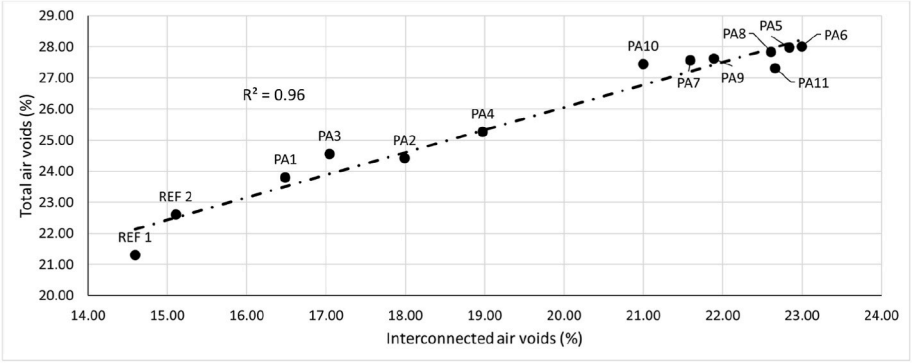

Fig. 5. Stretch relationship found between total and interconnected air voids.

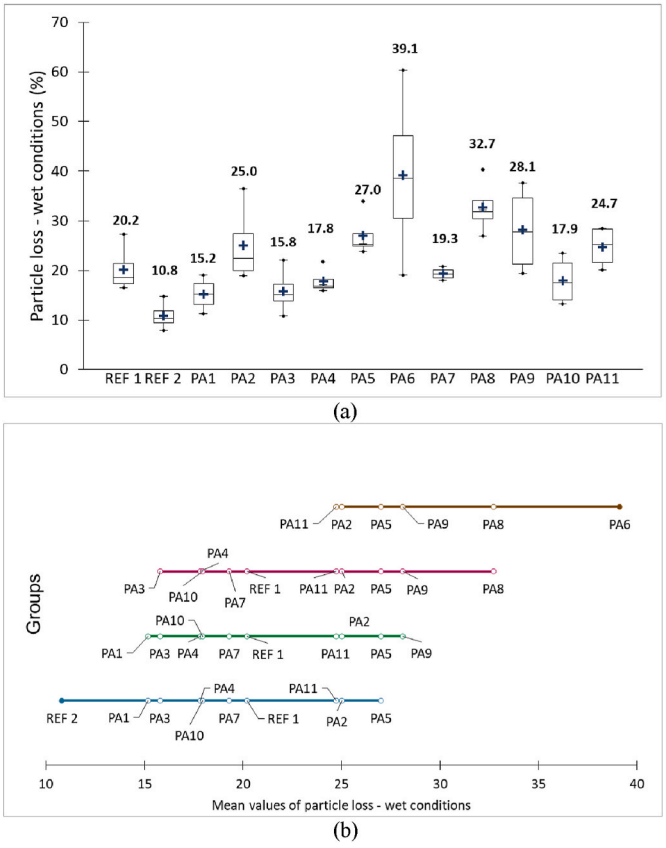

Fig. 7. Particle loss – wet conditions results; box and whiskers plot (a); Demsar plot (b).

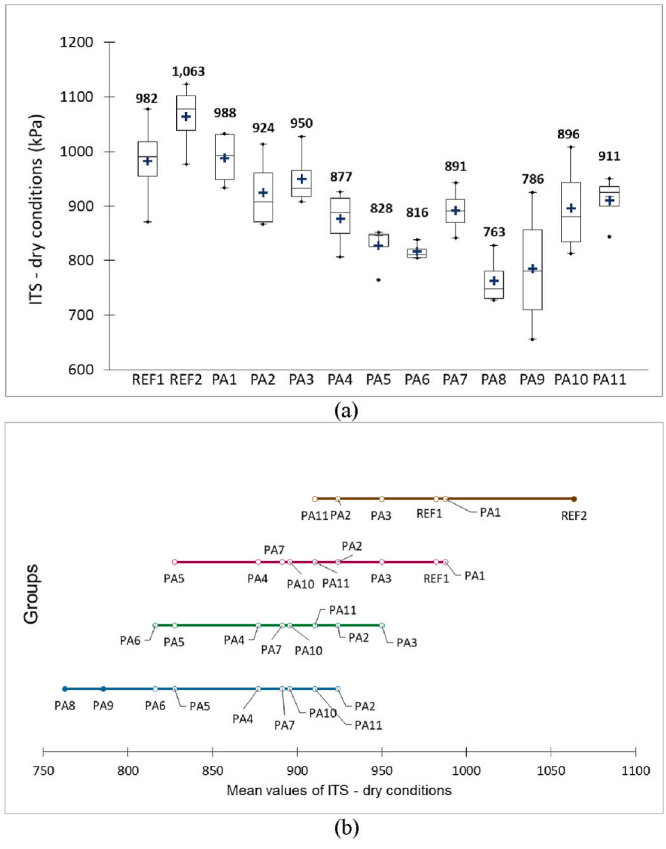

Fig. 8. ITS – dry conditions results; box and whiskers plot (a); Demsar plot (b).

Concerning the ITS at wet conditions, none of the experimental mixes could reach the same performance than the reference mix with modified binder. Like for particle loss, it is clearly observed that the mixes having more voids are more prone to fail under the action of water. In other words, mixtures with greater porosity are highly exposed to oxidation and aging and have less stone-on-stone contacts inside the structural skeleton of the porous asphalt. Despite this, the designs PA10 and PA11 showed a similar performance to the conventional REF1 mixture with no statistical differences (see Fig. 9b).

Concerning moisture sensitivity results (see Fig. 10), designs from 8 to 11 displayed good values of moisture resistance. Mixes PA8, PA9, PA10 displayed ITSR rates higher than 85%, fulfilling the requirements specified in the Spanish normative. In addition, PA11 showed a good ITSR value of 83%. Although it did not reach the minimum required value, it was the mixture with the highest void content, and obtained the best tensile strength in dry and wet conditions.

3.5. PCA and AHC exploratory analysis

As mentioned previously, with the exploratory analysis the aim is to visualize the correlation between the response variables and similarities between the experimental designs. Total and interconnected air voids, particles loss (dry and wet) and tensile strength (dry and wet) were the variables into consideration. Binder drain down was discarded as response variable since no mix presented binder drainage. The moisture sensitivity was also discarded because it is strictly dependent on the indirect tensile strength test. Thus, the PCA assesses the correlation between the variables. The PCA type was correlation matrix through the Pearson correlation coefficient due to the distribution of the data set. Accordingly, the results can be observed in the matrix plot (see Fig. 11). The histogram of the variables is displayed in the diagonal, while the

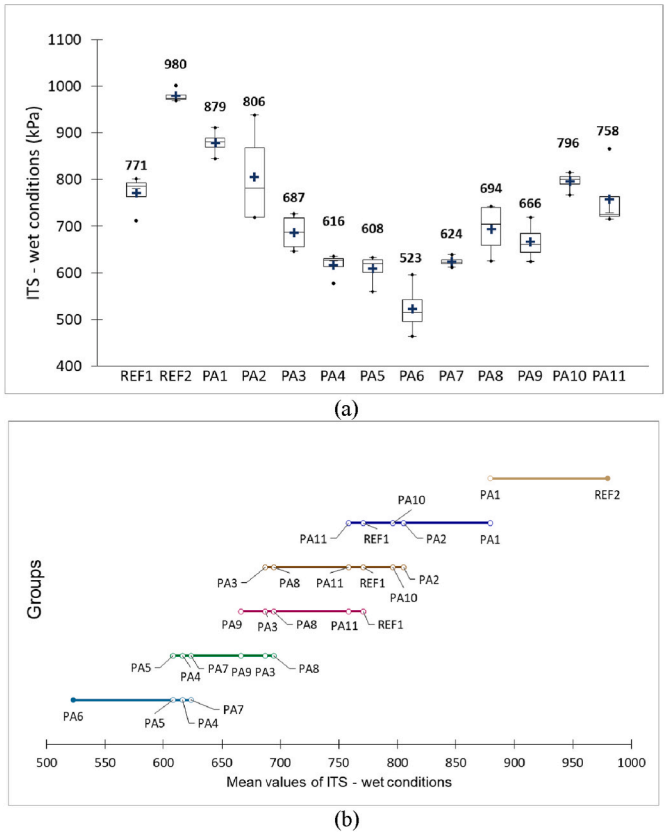

Fig. 9. ITS – wet conditions results; box and whiskers plot (a); Demsar plot (b).

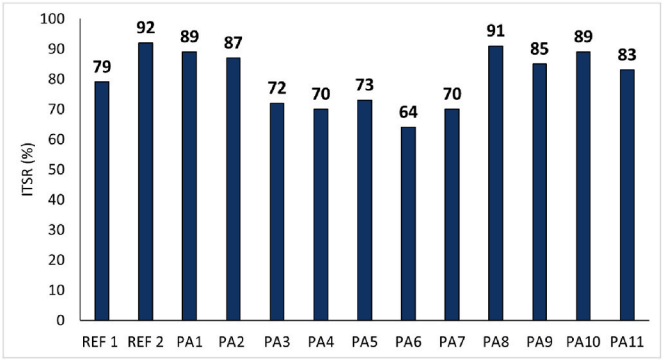

Fig. 10. Indirect tensile strength ratio (ITSR) results.

scatter plots show the combination among the variables. The red and blue color observed in the data points depicts if there is a positive or negative correlation, respectively. Meanwhile, the lines in the scatter plots reveal the pattern and stretch relationship between the response variables. For instance, the higher porosity values, the greater is the particle loss (red points). Similarly, as the air voids content increases, the tensile strength is lower (blue lines).

Subsequently, the original dimensionality of the feature space is reduced by mapping out in a smaller space whose axes are represented by factors (F) or principal components. In other words, PCA is computed as linear orthogonal transformation of the data set and response variables into a new coordinated system (Ghasemi et al., 2018). The first PC possesses the strongest variance along its axis followed by the second and third PCs and so on. As it can be observed in the scree plot of the PCA (Fig. 12), the response variables can be reduced in two factors with more than 80% of the data variance explained according to the eigenvalues. The eigenvalues reflect the quality of information contained in the variables of the data set to a smaller number of factors. For instance, the first factor explains 76% of the variability contained in the data.

Although it is typical to consider the first two factors to describe the multivariate dataset (Margaritis et al., 2020), in this study the third factor was taken instead of the second one because of the squared cosine values and because F3 loadings represent better the ITSwet and air voids response variables. The higher squared cosine, the larger the link with the corresponding axis. Fig. 13 shows the clustering tree or dendrogram, calculated from the AHC. The Ward's minimum variance method was

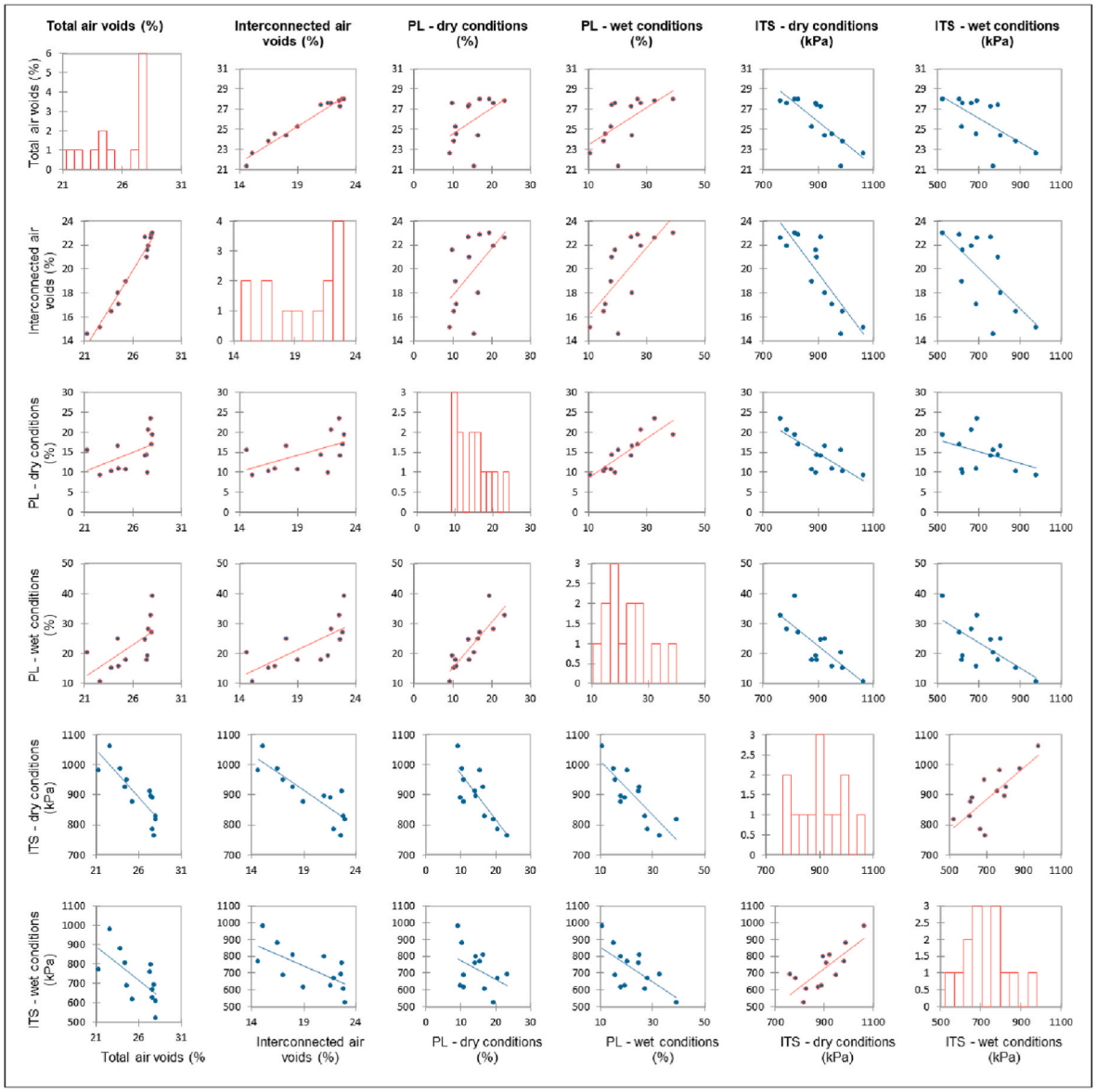

Fig. 11. Matrix plot of the response variables.

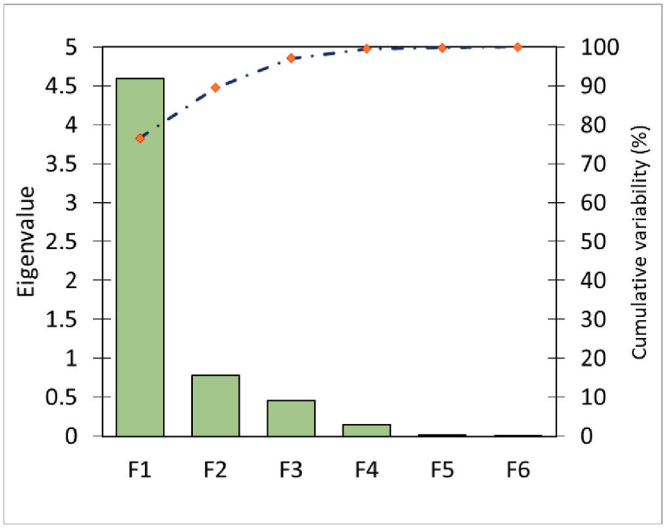

Fig. 12. Scree plot of the factors of the PCA.

the criterion applied in the hierarchical clustering analysis. As it can be seen, the dendrogram represents the progressive grouping of the observations and the dotted line indicates the level of truncation that has been considered. Based on the visual inspection of the derived clustering tree, the experimental PA mixtures were divided into five groups represented in five different colors. Each color group of observations is more homogeneous as compared to the others. From right to left. Yellow cluster: designs REF1 and PA2. Purple cluster: designs REF2 and PA1. Green cluster: designs PA7, PA10 and PA11. Red cluster: designs PA3 and PA4. Blue cluster: designs PA6, PA5, PA8 and PA9.

In the same way, the experimental designs are represented in the PCA space biplot (see Fig. 14). Based on the results, the first and third dimensions (F1 and F3) of the PCA display 76.62% and 7.60% of the total variance contained in the dataset respectively, reaching a cumulative variance of 84.22% and accomplishing 80% variance criterion as suggested in previous studies (Gabriel et al., 2020; Margaritis et al., 2020). The obtuse angles formed in the first four criteria (air voids and particle loss) entail positively linked variables. Smaller obtuse angles, the higher correlation among the criteria. For example, total and interconnected air voids are highly correlated as well as the particle loss in both dry and wet conditions presents a closer relationship. Indirect

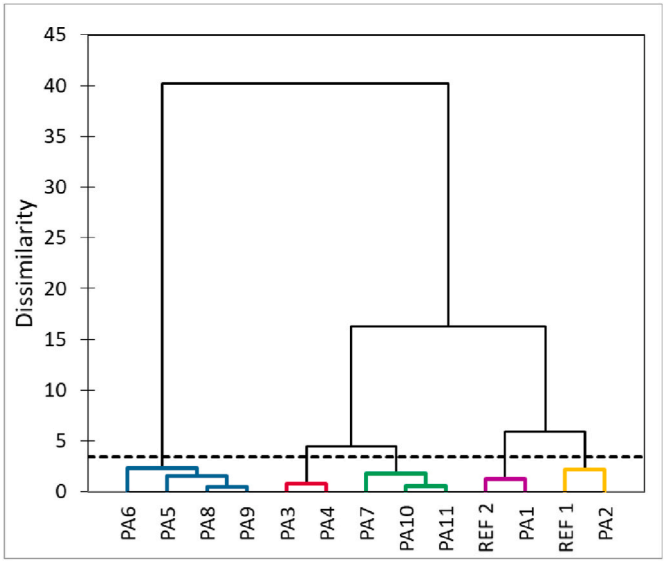

Fig. 13. Dendrogram plot of the PA experimental designs.

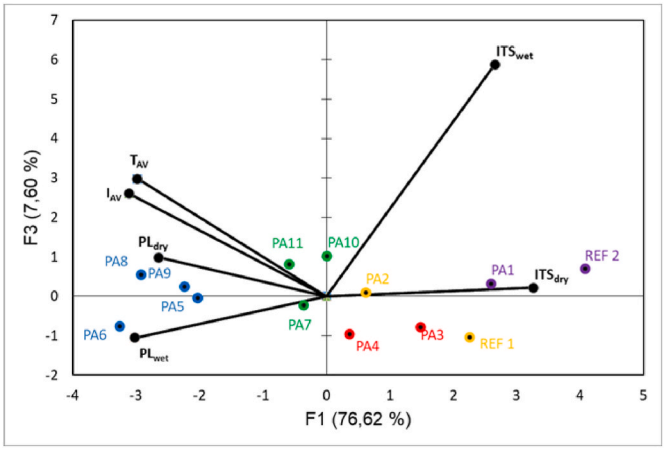

Fig. 14. Schematic two-dimensional map of the PCA analysis.

tensile strength response variables are on the opposite side of the center which indicates that they are significantly negatively correlated. This result was expected since the higher voids content, the lower the tensile strength. Similarly, the results shown a negative correlation between tensile strength and raveling, the lower the tensile strength, the greater is the particle loss. The experimental designs were also plotted in the schematic two-dimensional map as the goal of the PCA to identify trends. Based on the position of the individuals in the space biplot, designs contained in the blue cluster are driven towards high porosity values but low raveling resistance in both conditions. Purple and yellow clusters which embrace the first four experimental designs, are associated with the positive side of the PC1 which is defined by the tensile strength response. These mixtures displayed suitable values of durability but not the high porosity level as expected. Designs PA7, PA10 and PA11 located in the center of the space biplot were classified in the same group. Their positions on the map suggest that there is no bias towards any response variable. The three mixes displayed notable air voids levels with an adequate raveling resistance and tensile strength as compared to reference mixtures. Moreover, the dendrogram suggests that red and green clusters as well as purple and yellow groups could be merged if a higher cut-off line would be chosen. The pattern shows that the similarity between clusters is inter-related with the mechanical properties and that the main difference lies on the porosity.

4. Conclusions

The main aim of this study was the development of improved PA mixtures with higher air void contents and with a suitable structural capacity. Various experimental PA mixes with different gradations curves and modified with novel additives were progressively assessed to increase the porosity while maintaining a proper durability. The tests performed included total and interconnected air voids, binder drain down, particle loss both in dry and wet conditions, indirect tensile strength, and moisture susceptibility. Descriptive statistics were used to explore the basic features of the dataset, whereas inferential statistics were conducted to quantitatively compare the experimental designs. Additionally, PCA and AHC was incorporated to deal with the multivariate data analysis. The main findings are summarized as follows:

- The proposed PA mixes reached total air voids content between the range of 27–28% with an interconnected porosity of 22–23%. Strictly speaking, the interconnected porosity of the experimental mixes matches the same level of the total porosity of the reference mixtures.
- Regarding raveling resistance, proposed PA mixes displayed particle loss values lower than 20% and 35%, the threshold recommended according to Spanish normative for the highest traffic level at both dry and wet conditions, respectively.

- For the ITS results, the improved PA11 mixture showed similar tensile resistance at dry conditions as compared to reference mixtures with no statistically significant differences. At wet conditions, this mix did not reach the performance of the reference mixture with PMB. However, it maintained a performance similar to that of a conventional mixture with VB. Likewise, the moisture susceptible results of PA8, PA9, PA10 and PA11 were admissible since they displayed ITSR values closer to 85%, the requirement specified in the Spanish normative.
- The inclusion of fibers was significant in the performance of experimental PA mixes since they provided efficient reinforcement, improving the durability of the mixture and acted as stabilizer limiting binder drainage. Both types of fibers work well in terms of the overall performance. The addition of hydrated lime as a filler replacement also contributed to reduce stripping and increase raveling resistance and tensile strength in wet conditions.
- PCA and AHC demonstrated to be an efficient method in the exploratory analysis. PCA technique contributed to swiftly envision and analyze the correlations between the response variables and to visualize the observations in a low dimensional map based on an optimal view for variability criterion. Meanwhile, AHC helped to classify the individuals and grouped them in clusters according to the similarities found in their characteristics. As clearly illustrated, five clusters were identified among the PA mixtures. The inclusion of this method could facilitate the decision-making process when large amount of data sets is involved.

In conclusion, this research produced PA mixes with enhanced porosity and proper mechanical performance. The green cluster, composed by experimental designs PA7, PA10 and PA 11 were listed as the most promising alternatives. The use of PMB, fibers and HL was essential in the formulation of these mixes. Despite the auspicious results obtained from the investigation, further research incorporating other additives and additional experimental testing is recommended to explore the potential use of PA mixtures with high AV content in various traffic conditions.

Funding

This publication is part of the I+D+I projects PID2019-110797RB-I00 and PDC2021-120824-I00, funded by MCIN/AEI/10.13039/501100011033 and Unión Europea NextGenerationEU/PRTR".

Declaration of competing interest

The authors declare that they have no known competing financial interests or personal relationships that could have appeared to influence the work reported in this paper.

Data availability

Data will be made available on request.

Acknowledgments

The authors gratefully acknowledge the support of Teijin Aramid B. V. and Forta Corporation for their providing the different fibres.

References

Abtahi, S.M., Sheikhzadeh, M., Hejazi, S.M., 2010. Fiber-reinforced asphalt-concrete - a review. Construct. Build. Mater. 24 (6), 871–877. https://doi.org/10.1016/j.conbuildmat.2009.11.009.

Adam, J.F., Brooker, A.C., Carpenter, S.H., John, A.D., Huber, G., Jackson, D.C., Krugler, P.E., Lee, D., Mcdaniel, R.S., Mellott, D.B., Moulthrop, J.S., Shuler, S., Stroup-gardiner, M., Tam, K.K., 1998. OPEN-GRADED friction course: state of the practice. In: Transportation Research Circular E-C005. Transportation Research Circular E-C005, p. 20. December.

Alvarez, A.E., Martin, A.E., Estakhri, C., 2011. A review of mix design and evaluation research for permeable friction course mixtures. Construct. Build. Mater. 25 (3), 1159–1166. https://doi.org/10.1016/j.conbuildmat.2010.09.038.

Arrieta, V.S., Maquilón, J.E.C., 2014. Resistance to degradation or cohesion loss in Cantabro test on specimens of porous asphalt friction courses. Procedia - Soc. Behav. Sci. 162 (Panam), 290–299. https://doi.org/10.1016/j.sbspro.2014.12.210.

Bouayad, D., Emeriault, F., 2017. Modeling the relationship between ground surface settlements induced by shield tunneling and the operational and geological parameters based on the hybrid PCA/ANFIS method. Tunn. Undergr. Space Technol. 68, 142–152. https://doi.org/10.1016/j.tust.2017.03.011. November 2016.

Burgas, L., Colomer, J., Melendez, J., Gamero, F.I., Herraiz, S., 2021. Integrated Unfold-PCA Monitoring Application for Smart Buildings : an AHU Application Example.

Cadot, Y., Thiollet-scholtus, M., Samson, A., Barbeau, G., Cheynier, V., 2012. Characterisation of Typicality for Wines Related to Terroir by Conceptual and by Perceptual Representations . An Application to Red Wines from the Loire Valley. https://doi.org/10.1016/j.foodqual.2011.08.012. April.

Calzada-Perez, M.A., Perez-Jimenez, F.E., 1984. Desarrollo y normalización del ensayo de pérdida por desgaste aplicado a la caracterización, dosificación y control de mezclas bituminosas de granulometría abierta. Universidad de Cantabria.

Canal, B.M., Delta, E.N., 2020. Multivariate Analysis for Assessing Irrigation Water Quality : A Case Study of the Multivariate Analysis for Assessing Irrigation Water Quality : A Case Study of the Bahr Mouise Canal , Eastern Nile Delta. https://doi.org/10.3390/w12092537. September.

Chen, J., Yao, C., Wang, H., Ding, Y., Xu, T., 2018a. Expansion and contraction of clogged open graded friction course exposed to freeze-thaw cycles and degradation of mechanical performance. Construct. Build. Mater.

Chen, J., Yin, X., Wang, H., Ding, Y., 2018b. Evaluation of durability and functional performance of porous polyurethane mixture in porous pavement. J. Clean. Prod. 188, 12–19. https://doi.org/10.1016/j.jclepro.2018.03.297.

Elshamy, A.I., Mohamed, T.A., Essa, A.F., Abd-elgawad, A.M., 2019. *Recent Advances in Kaempferia Phytochemistry and Biological Activity : A Recent Advances in Kaempferia Phytochemistry and Biological Activity : A Comprehensive Review* (Issue October). https://doi.org/10.3390/nu11102396.

Fazaeli, H., Samin, Y., Pirnoun, A., Dabiri, A.S., 2016. Laboratory and field evaluation of the warm fiber reinforced high performance asphalt mixtures (case study Karaj – Chaloos Road). Construct. Build. Mater. 122, 273–283. https://doi.org/10.1016/j.conbuildmat.2016.05.139.

Gabriel, R., Valeriu, C., Ro, B., Vornicu, N., Stanc, S., 2020. Catena Soil Spatial Patterns Analysis at the Ancient City of Ibida (Dobrogea , SE Romania), via Portable X-Ray Fl Uorescence Spectrometry and M ultivariate Statistical Methods, vol. 189, pp. 1–12. https://doi.org/10.1016/j.catena.2020.104506. February.

Garcia, A., Aboufoul, M., Asamoah, F., Jing, D., 2019. Study the influence of the air void topology on porous asphalt clogging. Construct. Build. Mater. 227, 116791 https://doi.org/10.1016/j.conbuildmat.2019.116791.

Ghasemi, P., Aslani, M., Rollins, D.K., 2018. Principal Component Analysis-Based Predictive Modeling and Optimization of Permanent Deformation in Asphalt Pavement : Elimination of Correlated Inputs and Extrapolation in Modeling.

Gupta, A., Castro-fresno, D., Lastra-gonzalez, P., Rodriguez-hernandez, J., 2021a. Selection of fibers to improve porous asphalt mixtures using multi-criteria analysis. Construct. Build. Mater. 266, 121198 https://doi.org/10.1016/j.conbuildmat.2020.121198.

Gupta, A., Rodriguez-Hernandez, J., Castro-Fresno, D., 2019. Incorporation of additives and fibers in porous asphalt mixtures: a review. Materials 12 (19), 3156. https://doi.org/10.3390/ma12193156.

Gupta, A., Slebi-Acevedo, C.J., Lizasoain-Arteaga, E., Rodriguez-Hernandez, J., Castro-Fresno, D., 2021b. Multi-criteria selection of additives in porous asphalt mixtures using mechanical, hydraulic, economic, and environmental indicators. Sustainability 13 (4), 1–21. https://doi.org/10.3390/su13042146.

Hammes, G., Thives, L.P., Ghisi, E., 2018. Application of stormwater collected from porous asphalt pavements for non-potable uses in buildings. J. Environ. Manag. 222, 338–347. https://doi.org/10.1016/j.jenvman.2018.05.094.

Hu, Y., Cheng, F., Ji, Y., Yuan, B., Hu, X., 2020. Effect of aramid pulp on low temperature flexural properties of carbon fibre reinforced plastics. Compos. Sci. Technol. 192, 108095 https://doi.org/10.1016/j.compscitech.2020.108095.

Huurman, R.M., Mo, L., Woldekidan, M.F., 2010. Unravelling porous asphalt concrete towards a mechanistic material design tool. Road Mater. Pavement Des. 11 (3), 583–612. https://doi.org/10.1080/14680629.2010.9690295.

Lertwassana, W., Parnklang, T., Mora, P., Jubsilp, C., Rimdusit, S., 2019. High performance aramid pulp/carbon fiber-reinforced polybenzoxazine composites as friction materials. Compos. B Eng. 177, 107280 https://doi.org/10.1016/j.compositesb.2019.107280.

Liu, M., Huang, X., Xue, G., 2016. Effects of double layer porous asphalt pavement of urban streets on noise reduction. Int. J. Sustain. Built Environ. 5 (1), 183–196. https://doi.org/10.1016/j.ijsbe.2016.02.001.

Lyons, K.R., Putman, B.J., 2013. Laboratory evaluation of stabilizing methods for porous asphalt mixtures. Construct. Build. Mater. 49, 772–780. https://doi.org/10.1016/j.conbuildmat.2013.08.076.

Ma, X., Li, Q., Cui, Y.-C., Ni, A.-Q., 2018. Performance of porous asphalt mixture with various additives. Int. J. Pavement Eng. 19 (4), 355–361. https://doi.org/10.1080/10298436.2016.1175560.

Manrique-Sanchez, L., Caro, S., Arámbula-Mercado, E., 2018. Numerical modelling of ravelling in porous friction courses (PFC). Road Mater. Pavement Des. 19 (3), 668–689. https://doi.org/10.1080/14680629.2016.1269661.

Margaritis, A., Road, B., Soenen, H., Fransen, E., Pipintakos, G., 2020. Identification of Ageing State Clusters of Reclaimed Asphalt Binders Using Principal Component Analysis (PCA) and Hierarchical Cluster Analysis (HCA) Based on Chemo-Rheological Parameters. https://doi.org/10.1016/j.conbuildmat.2020.118276. February.

Mo, L.T., Huurman, M., Wu, S.P., Molenaar, A.A.A., 2011. Bitumen – Stone Adhesive Zone Damage Model for the Meso-Mechanical Mixture Design of Ravelling Resistant Porous Asphalt Concrete, vol. 33, pp. 1490–1503. https://doi.org/10.1016/j.ijfatigue.2011.06.003.

Mohd Shukry, N.A., Hassan, N.A., Abdullah, M.E., Hainin, M.R., Md Yusoff, N.I., Jaya, R. P., Mohamed, A., 2018. Effect of various filler types on the properties of porous asphalt mixture. IOP Conf. Ser. Mater. Sci. Eng. 342 (1) https://doi.org/10.1088/1757-899X/342/1/012036.

Nielsen, C., 2006. Durability of Porous Asphalt-International Experience. *Technical Note 41 Copenhagen, Denmark: Danish Road Institute (DRI)*.

Park, P., El-Tawil, S., Park, S.Y., Naaman, A.E., 2015. Cracking resistance of fiber reinforced asphalt concrete at -20 °c. Construct. Build. Mater. 81, 47–57. https://doi.org/10.1016/j.conbuildmat.2015.02.005.

Putman, B.J., Asce, A.M., Kline, L.C., 2012. Comparison of Mix Design Methods for Porous Asphalt Mixtures, vol. 24, pp. 1359–1367. https://doi.org/10.1061/(ASCE)MT.1943-5533.0000529. November.

Ranieri, V., Sansalone, J.J., Shuler, S., Ranieri, V., Sansalone, J.J., Shuler, S., David, V.R., 2011. Relationships Among Gradation Curve , Clogging Resistance , and Pore-Based Indices of Porous Asphalt Mixes Relationships Among Gradation Curve , Clogging Resistance , and Pore-Based Indices of Porous Asphalt Mixes. https://doi.org/10.3166/RMPD.11HS.507-525, 0629.

Ren, S., Liu, X., Xu, J., Lin, P., 2021. Investigating the role of swelling-degradation degree of crumb rubber on CR/SBS modified porous asphalt binder and mixture. Construct. Build. Mater. 300, 124048 https://doi.org/10.1016/j.conbuildmat.2021.124048.

Rogers, D., Karan, P., Turner, I., Arnold, G., Alexander, D., 2019. Performance Benefits of Polymer Modified Bitumen Binders for Thin Surfacings.

Slebi-Acevedo, C.J., Castro-Fresno, D., Pascual-Muñoz, P., Lastra-González, P., 2021. A combination of DOE–multi-criteria decision making analysis applied to additive assessment in porous asphalt mixture. Int. J. Pavement Eng. 0 (0), 1–14. https://doi.org/10.1080/10298436.2020.1859508.

Slebi-Acevedo, C.J., Castro-Fresno, D., Pascual-Muñoz, P., Lastra-González, P., 2022. A combination of DOE – multi-criteria decision making analysis applied to additive assessment in porous asphalt mixture. Int. J. Pavement Eng. 23 (8), 2489–2502. https://doi.org/10.1080/10298436.2020.1859508.

Slebi-Acevedo, C.J., Lastra-González, P., Castro-Fresno, D., Bueno, M., 2020. An experimental laboratory study of fiber-reinforced asphalt mortars with polyolefin-aramid and polyacrylonitrile fibers. Construct. Build. Mater. 248, 118622 https://doi.org/10.1016/j.conbuildmat.2020.118622.

Slebi-acevedo, C.J., Lastra-gonzález, P., Indacoechea-vega, I., Castro-fresno, D., 2020. Laboratory assessment of porous asphalt mixtures reinforced with synthetic fibers. Construct. Build. Mater. 234 https://doi.org/10.1016/j.conbuildmat.2019.117224.

Tidjani, A., Redondin, M., Bouillaut, L., Daucher, D., 2020. Impact of Road Infrastructure Characteristics on Road Markings. https://doi.org/10.3850/981-973-0000-00-0.

Xu, B., Chen, J., Li, M., Cao, D., Ping, S., Zhang, Y., Wang, W., 2016. Experimental investigation of preventive maintenance materials of porous asphalt mixture based on high viscosity modified bitumen. Construct. Build. Mater. 124, 681–689. https://doi.org/10.1016/j.conbuildmat.2016.07.122.

Xu, Q., Chen, H., Prozzi, J.A., 2010. Performance of fiber reinforced asphalt concrete under environmental temperature and water effects. Construct. Build. Mater. 24 (10), 2003–2010. https://doi.org/10.1016/j.conbuildmat.2010.03.012.